Upgrading catalytic activity of NiO/CaO/MgO from natural limestone as catalysts for transesterification of coconut oil to biodiesel

Nuni Widiarti[1] · Hasliza Bahruji[2] · Holilah Holilah[1] · Yatim Lailun Ni'mah[1] · Ratna Ediati[1] · Eko Santoso[1] · Aishah Abdul Jalil[3] · Abdul Hamid[4] · Didik Prasetyoko[1]

Abstract

Limestone was converted to high surface area CaO/MgO catalysts via calcination-hydration-dehydration (CHD) method for transesterification of coconut oil to biodiesel. Thermal decomposition at 900°C transformed dolomite $CaMg(CO_3)_2$ to large crystallite and low surface area CaO/MgO. CHD treatment eliminated the large CaO/MgO aggregates and increased the surface area and the activity of CaO/MgO. The addition of polyethylene glycol (PEG) as surfactant during CHD reduced the CaO/MgO crystallite size to ~377 nm and enhanced the surface area (39 m^2/g), the pore volume (0.0322 m^3/g), and the basicity of the catalysts (7.8 mmol/g). Transesterification of coconut oil showed an increase in oil conversion from 16.45 to 49.27% when CaO/MgO was produced using PEG. Optimization studies at the variation of reaction temperatures, the ratio methanol:oil, and the amount of catalysts produced the optimum biodiesel yield of 81.76%. Impregnation with 5% NiO introduced acid-base functionality for esterification FFA to FAME, further improved biodiesel yield to 90%, and reduced the FFA yield. The kinematic, density, flash point, acid numbe,r and carbon residue of biodiesel from coconut oil were determined at 1.93 mm^2/s, 0.86g/cm^3, 137°C, 0.27 mg KOH/g, and 0.22% respectively, and were within the ASTM D6751 standard.

1 Introduction

The global energy crisis has opened up opportunities for researcher to investigate the production of sustainable and renewable source of energy such as solar and wind energy, hydrogen, and fuel from biomass [1, 2]. Biodiesel from biomass provided a green and non-toxic alternative, classified as sustainable, renewable, and environmental friendly fuel [3–6].

Statement of novelty This study aimed to enhance the catalytic activity of CaO/MgO from limestone as naturally abundant minerals without removal of MgO for transesterification reaction. Direct decomposition of limestone produced CaO/MgO with low catalytic activity. Calcination-hydration-dehydration (CHD) treatment on limestone with the addition of surfactant have reduced the crystallite size and enhanced the surface area, the pore volume, and the basicity for high activity towards biodiesel production. Following impregnation with 5% NiO, the activity of CaO/MgO was increased for the production of biodiesel and significantly reduced the FFA formation. NiO introduced acid-base functionality to the catalysts for efficient esterification of free fatty acids to methyl esters.

✉ Didik Prasetyoko
didikp@chem.its.ac.id; didik.prasetyoko@gmail.com

[1] Department of Chemistry, Faculty of Science and Data Analytics, Institut Teknologi Sepuluh Nopember, Surabaya 60111, Indonesia

[2] Centre of Advanced Material and Energy Sciences, Universiti Brunei Darussalam, Jalan Tungku Link, BE 1410, Brunei

[3] Department of Chemical Engineering, Universiti Teknologi Malaysia (UTM), 81310 Johor Bahru, Johor, Malaysia

[4] Department of Heavy Equipment Mechanical Engineering, Politeknik Negeri Madura, Madura, East Java, Indonesia

Biodiesel consists of a mixture of alkyl esters from long-chain fatty acids [7–9] with better lubricating properties and low sulfur content in comparison to fossil fuels [10, 11]. Triglyceride from vegetable oil or animal lipid was transformed via transesterification reaction with alcohol (methanol or ethanol) to produce methyl esters [12–14]. Ideally, catalysts for transesterification must be easily separated from the product, non-corrosive and stable against deactivation, or further reaction with reactant or product [15, 16].

CaO has been investigated as catalyst for biodiesel production due to the high basicity, non-toxicity, and eco-friendly properties [1, 9]. CaO was generally produced from decomposition of $CaCO_3$ at high temperatures between 600 and 1000°C [9, 17, 18]. $CaCO_3$ can be extracted from many natural substances such as limestone[19], chicken eggshells[20], and shellfish[21], and was even found in chicken manure[10]. Limestone is an abundantly available mineral mainly consisted of Ca and Mg in the form of dolomite $CaMg(CO_3)_2$. CaO catalysts derived from natural limestone via thermal decomposition and co-precipitation method showed high activity for transesterification reaction in comparison to MgO and CaO/MgO composites [19]. However, extraction of CaO from dolomite required a precise control of the temperatures [22] or the use of strong acid to facilitate the leaching process of Mg [23]. Although the activity of CaO/MgO from dolomite was lower than the isolated CaO[19], the presence of MgO enhanced the basicity and the stability of CaO towards deactivation in the presence of free fatty acids in oil [24, 25]. Conversion of dolomite to CaO/MgO was carried out using direct calcination at high temperatures; however, the CaO/MgO formed large crystallites with low surface area which was proven detrimental towards the activity of the catalysts[26]. Surfactants such as cetyltrimethylammonium bromide (CTAB) and polyethylene glycol (PEG) have been widely employed for the synthesis of catalysts to enhance dispersion of solid particles, thermal stability, and porosity [27]. The porosity of metal oxide was developed by the self-assembly of surfactants molecule in the solid solution [28]. Large molecular weight PEG created a stable bond with Ca^{2+} for the formation of small CaO particles [29]. CTAB was also reported to form uniform particles due to the enhanced viscosity of the solution preventing interaction between ions and therefore enhanced the dispersion [30].

This research aimed to upgrade the catalytic activity of CaO/MgO from limestone as naturally abundant mineral for transesterification of coconut oil to biodiesel via calcination-hydration-dehydration (CHD) method. Cationic surfactant cetyltrimethylammonium bromide (CTAB) and non-ionic surfactant polyethylene glycol (PEG) were added during CHD in order to control the recrystallization process. Crystallite size, surface area, porosity, and basicity of CaO/MgO were correlated with the oil conversion and the selectivity towards methyl esters. Biodiesel production was optimized by the variation of the amount of catalysts, the ratio between

methanol and oil and the influence of reaction temperatures. The effect of NiO nanoparticles on the catalytic activity of CaO/MgO was investigated with the variation of NiO loading and finally the biodiesel properties were also determined according to the ASTM standard.

2 Materials and methods

2.1 Materials

Limestone was obtained from Madura, East Java, Indonesia. Ammonia 25% (Merck), benzoic acid 99% (Merck), cetyltrimethylammonium bromide (CTAB) 98% (Sigma Aldrich), hydrochloric acid 37% (Merck), methanol 99,9% (Merck), n-hexane 99% (Merck), polyethylene glycol (PEG 1000) (Merck), Hammett indicator (phenolphthalein (Sigma Aldrich), 2,4-dinitroaniline (Sigma Aldrich), and 4-nitroaniline (Sigma Aldrich), and distilled water.

2.2 Catalyst preparation

The calcination-hydration-dehydration (CHD) method was carried out by crushing Madura limestone into 125 mesh and washed with water until the pH of the filtrate reached 7. The limestone powder was then dried at 110 °C for 12 h and calcined at 900 °C for 3 h to form CaO/MgO. The calcined CaO/MgO was rehydrated by mixing with distilled water, sonicated at 60 °C for 150 min and then was placed under microwaves at 400 watts for 10 min. Finally, the dehydration process was carried on CaO/MgO powder via hydrothermal method with the presence of surfactant CTAB and PEG. For dehydration using CTAB surfactant labeled as CaO/MgO-C, 5.028 g CTAB was dissolved with 100 ml distilled water followed by the addition of 4.48 g of CaO/MgO powder and continued to stir for 3 h at 60 °C. For dehydration using PEG surfactant labeled as CaO/MgO-P, similar approached was repeated but using 13.79 g of PEG. The mixture was put into a hydrothermal reactor and heated at 160 °C for 24 h. Next, the solids obtained were filtered and the precipitates were washed with water until the pH of the filtrate becomes neutral. The solid was also washed with copious amount of ethanol to remove the excess surfactants. Calcination was carried out on the resulting powder in a tubular furnace at 800 °C for 3 h. The process was also repeated following the similar procedures without the presence of surfactants and labeled as CaO/MgO-H.

2.3 Catalyst characterization

Analysis of the composition of limestone was carried out using XRF (Philips Xpert MPD). Thermal stability of limestone was analyzed using thermo-gravimetric analyzer (TGA) Linseis STA PT-1000 at room temperature until 900 °C, 10°

per minute of heating rate. The crystallinity and the mineral phases were determined using PHILIPS binary (scan) PW 3050/60 X-ray diffractometer, with Cu Kα radiation and generator settings of 30 mA and 40 kV. Particle size was measured using Zetasizer nm (Malvern). The morphology was investigated using JEOL JSM 6010LV scanning microscope at an accelerated voltage of 10 kV. The catalyst functional group was characterized using Fourier transform infrared (FTIR 8400S Shimadzu) with a KBr/pellet ratio of 99 mg/1 mg and measured at 400–4000 cm^{-1}. The surface area was calculated using N_2 adsorption-desorption technique, Quantachrome Physics instrument. The basicity of the catalyst was measured using the Hammett indicator. For analysis of the basicity strength, the catalyst was calcined at 800°C for 3 h and cooled down to 100°C. The catalyst was immediately removed from the furnace and dripped with Hammett indicator solution consisting of phenolphthalein, 2-nitroaniline and 4-nitroaniline in ethanol [13]. Meanwhile, the number of basic sites was determined using titration with benzoic acid solution. 0.15 g of freshly calcined catalyst was dispersed in toluene solution containing phenolphthalein (2 ml, 0.1 mg/ml) and stirred for 30 min. The solution was titrated with benzoic acid in toluene (0.01 M).

2.4 Catalytic activity

Transesterification of coconut oil to biodiesel was carried out in stainless steel autoclave with Teflon-liner equipped with magnetic stirrer and thermometer. Catalyst and methanol were mixed at 65°C in the reactor and stirred at 500 rpm. In another beaker, 50 mL of coconut oil was heated at 120°C. After the temperature was reached at 120°C for 10 min, the oil was put into the autoclave reactor and sealed. CaO/MgO, CaO/MgO-H, CaO/MgO-C, and CaO/MgO-P were used as catalysts respectively with the amount of catalysts were varied at 0.625, 1.25, 2.5, 3.75, and 5% wt/v. The compositions of oil to methanol were varied at 1:3, 1:6, 1:9, 1:12, and 1:15, and the reaction temperatures were changed at 100, 125, 15, and 175 °C.

2.5 Analysis properties of biodiesel

The properties of biodiesel including flash point, kinematic viscosity, density, acid number, and carbon residue were compared with the value according to the ASTM D6751 standard of bio-fuel. Determination of flash point was measured using ASTM D93 standard test method for flash point by Pensky-Martens Closed Cup Tester. The biodiesel was placed in a brass cup with cover, and an ignition source is directed into the test cup at regular intervals with stirring, until a flash is detected. Kinematic viscosity was determined by measuring the time for biodiesel to flow under gravity through a calibrated glass capillary viscometer at 40°C according to ASTM D-445 standard test method. Biodiesel density was carried out

following ASTM D-1298 method at 15°C and the acid number was determined using titration with a standard solution of 0.1 N KOH according to ASTM D-664. Carbon residue was measured by placing biodiesel sample in a glass vial and heated to 500°C under nitrogen atmosphere to evacuate the volatile compound and to decompose the biodiesel. The carbonaceous-type residue is reported as a percentage of the original sample (ASTM D4530)

Biodiesel composition was analyzed using GC-MS (Agilent Technologies 6820). Quantitative analysis of oil conversion was calculated using formula 1.

Oil conversion (%)

$$= \frac{\text{Weight of initial oil} - \text{weight of residual}}{\text{Weight of initial oil}} \times 100\%. \quad (1)$$

The selectivity and yield of FFA and biodiesel were then calculated according to the following Eqs. 2–4.

FAME selectivity (%)

$$= \frac{\text{Weight of FAME product}}{\text{Weight FAME} + \text{FFA}} \times 100\%. \quad (2)$$

Yield of FAME or biodiesel (%)

$$= \left(\frac{\sum A_{\text{FAME}}}{A_{\text{is}}} \right) \left(\frac{C_{\text{is}} \times V_{\text{is}}}{m_{\text{s}}} \right) \times 100\%. \quad (3)$$

$$\text{Yield of FFA (\%)} = \left(\frac{\sum A_{\text{FFA}}}{A_{\text{is}}} \right) \left(\frac{C_{\text{is}} \times V_{\text{is}}}{m_{\text{s}}} \right) \times 100\%. \quad (4)$$

where $\sum A$ is the number of areas under all peaks from fatty acid methyl ester (FAME) (C8:0 to C24:1); A_{IS} is the peak area of methyl heptadecanoate used as an internal standard; C_{IS} is the concentration of the methyl heptadecanoate solution (g mL^{-1}); V_{IS} is the volume of the methyl heptadecanoate (mL) solution; and m_{s} is the sample weight (mg) [17].

3 Results and discussion

3.1 Characterization of limestone using XRF and DTG/TGA analysis

XRF analysis was used to determine the elemental composition of limestone from Madura Island used as CaO/MgO precursor. Based on the XRF analysis, limestone contained 50.7% of Mg and 46.8% of Ca with traces amount of Fe (1.9%). TGA/DTG analysis was used to determine the thermal stability of limestone and the temperatures for evacuation of the volatile impurities [31]. Figure 1 showed the stability of limestone until 600°C followed by significant reduction of weight at ~39.21% between 700 and 800°C due to the decomposition of $CaMg(CO_3)_2$ to MgO, CaO, and CO_2. Initially
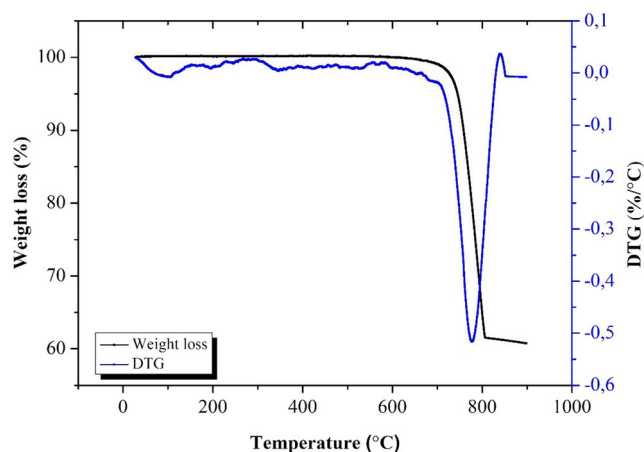
Fig. 1 DTG/TGA and DSC profiles of limestone from Madura Indonesia

dolomite was transformed to MgO and $CaCO_3$ (calcite) at 600–800°C followed by the decomposition of calcite to CaO and CO_2 at 740–800°C [32–34]. The sharp decomposition peak observed in TGA indicated the high crystalline order of dolomite that required calcination at 900 °C for complete transformation into CaO/MgO.

3.2 Characterization of CaO/MgO catalysts

3.2.1 XRD analysis

The transformation of limestone into CaO/MgO catalysts via CHD treatment with the presence of PEG and CTAB surfactants was recorded using XRD technique. XRD pattern of limestone (Fig. 2) showed the main peaks corresponded to $CaMg(CO_3)_2$ (dolomite) (JCPDS No. 00-083-1530). Following calcination at 900°C, the $CaMg(CO_3)_2$ peaks disappeared and the peaks associated with CaO were observed at $2\theta = 32°$, $37°$, and $55°$ (JCPDS No. 00-004-0777). Meanwhile, the MgO peak appeared at $2\theta = 43.7°$ was assigned to (200) crystal plane (JCPDS No. 01-077-2364). Calcination of limestone at 900°C also showed the presence of low intensity peaks at $2\theta = 29°$ (JCPDS No. 00-183-1762) corresponded to calcite ($CaCO_3$) and 18°, 34°, and 54.25° assigned to $Ca(OH)_2$ (JCPDS No. 00-084-1267) [10, 35]. CHD treatment of the CaO/MgO without the presence of surfactant showed the increase of $CaCO_3$ peak intensity due to the reaction of CaO with CO_2 in air, and $Ca(OH)_2$ peak intensity resulted from the reaction with moisture. Introduction of CTAB during CHD treatment inhibited the formation of calcite and $Ca(OH)_2$; meanwhile, PEG exhibited the increase intensity of calcite and $Ca(OH)_2$ peaks. PEG is a polyether polymer with hydroxyl group in the structure, which was largely decomposed into CO_2 and H_2O at high temperatures. During calcination, CaO was reacted with the resulting H_2O and CO_2 to form $CaCO_3$ and $Ca(OH)_2$ [36]. Strong hydrogen bond developed between the hydroxyl group in PEG with
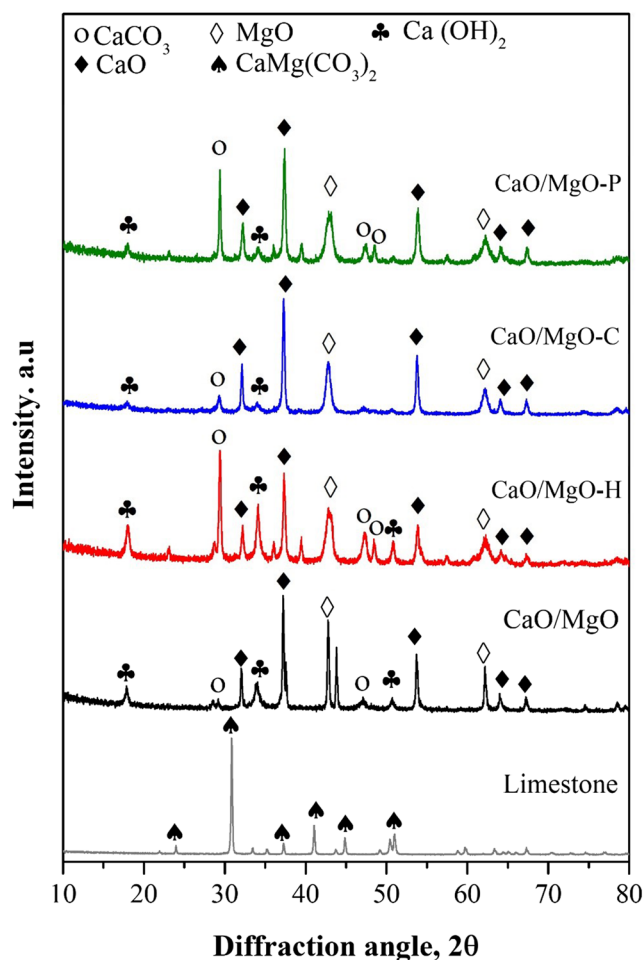


Fig. 2 XRD patterns of limestone, CaO/MgO, CaO/MgO-H, CaO/MgO-C, and CaO/MgO-P

CaO may also contribute to the formation of $Ca(OH)_2$ and $CaCO_3$. Nevertheless, there were no significant differences on the diffraction peaks of CaO/MgO-H, CaO/MgO-C, and CaO/MgO-P catalysts following CHD method apart from the intensity of $Ca(OH)_2$ and $CaCO_3$ peaks varied depending of the synthesis procedures.

3.2.2 Morphology and particle size analysis

SEM analysis of CaO/MgO produced from direct calcination of limestone revealed the formation of large crystallites with irregular morphology (Fig 3a). CHD method without the presence of surfactant significantly reduced the frequency of large aggregates to form much smaller crystallites (Fig 3b). Addition of CTAB and PEG to the CaO/MgO during CHD treatment further reduced the crystallite size of the catalysts. The CaO/MgO composites were also monitored using FESEM, (Fig 3e–h) to show the morphology of the small crystallites. The results of the FESEM analysis showed the formation of spherical shape CaO/MgOs with the appearances of small crystallites following addition of CTAB and PEG.
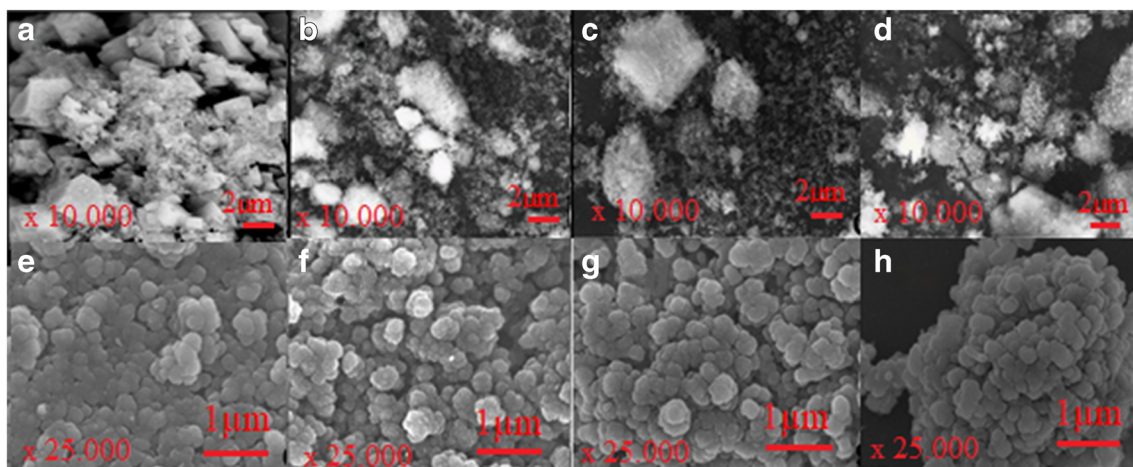
Fig. 3 SEM images of CaO/MgO (**a**), CaO/MgO-H (**b**), CaO/MgO-C (**c**), and CaO/MgO-P (**d**) and FESEM images of CaO/MgO (**e**), CaO/MgO-H (**f**), CaO/MgO-C (**g**), and CaO/MgO-P (**h**)

CaO/MgO catalysts were further analyzed using particle size analyzer and the crystallite size distributions were shown in Fig. 4. CaO/MgO produced from direct calcination of limestone showed the crystallites were divided into small aggregates with the average size of 0.426 μm and the large aggregates with the average size of 5.027 μm. The average diameter of CaO/MgO from direct calcination was determined at 0.681 μm. Following CHD treatment without the presence of surfactant, the crystallite size of CaO/MgO-H significantly reduced to give the average diameter of 0.521 μm, with the disappearances of the large aggregates >2 μm. The addition of CTAB surfactant showed the shift of CaO/MgO-C crystallite sizes to diameter less than 2 μm with the average diameter significantly reduced to 0.391 μm. CaO/MgO-P catalyst produced using PEG also showed further reduction of the average diameter to ~ 0.377 μm. In general, CHD treatment reduced the presence of large CaO/MgO crystallites due to the enhanced dispersion following hydration and dehydration methods. The crystallite size was further reduced with the addition of surfactants that prevented the agglomeration of CaO/MgO particles. The particle size reduced in the order of CaO/MgO > CaO/MgO-H > CaO/MgO-C > CaO/MgO-P.

Fig. 4 Particle size distribution of CaO/MgO, CaO/MgO-H, CaO/MgO-C, and CaO/MgO-P
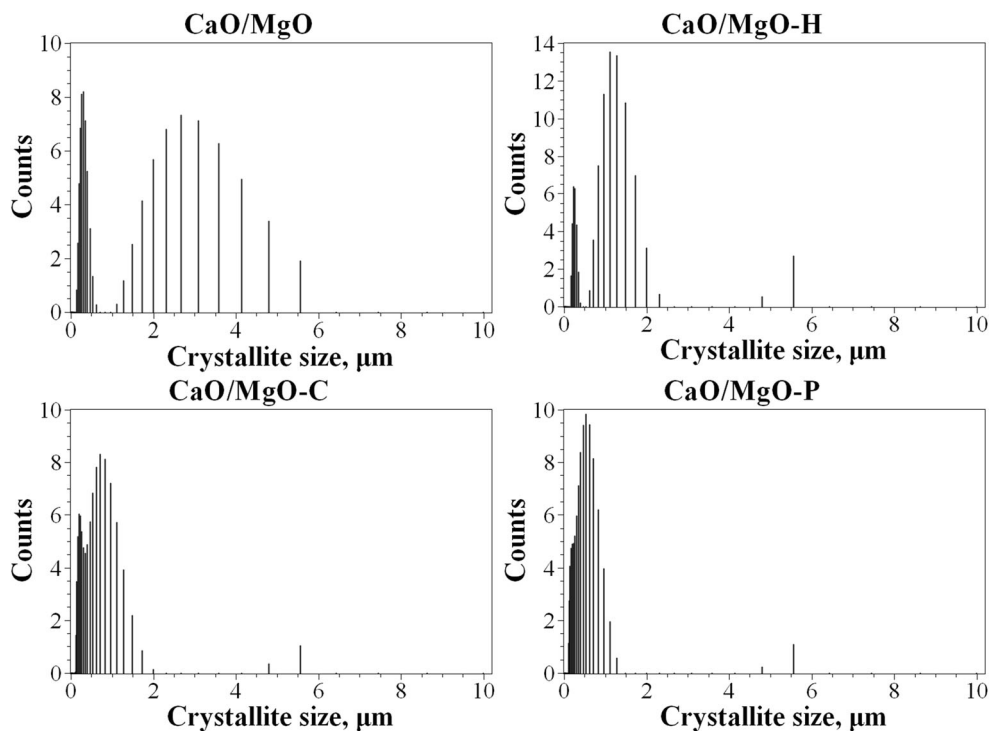
3.2.3 The basicity of the catalysts

The Hammett method was used to determine the basicity of the catalysts using phenolphthalein (H_ = 9.8), 2.4-dinitroaniline (H_ = 15.0), and 4-nitroaniline (H_ = 18.4) as indicators [13, 37, 38]. The results of the basicity analysis were summarized in Table 1. In general, all CaO/MgO have strong basicity with the basic strengths determined within $15 \leq$ (H_) ≤ 18.4 range. The analysis of the number of basic sites showed the increase of surface basicity of the catalysts was in the order of CaO/MgO-H < CaO/MgO-C < CaO/MgO-P < CaO/MgO. CHD treatment involved hydration and dehydration of CaO/MgO from the calcined limestone that caused reduction in basicity. PEG restored the basicity of CaO/MgO presumably due to the formation of calcium hydroxide clusters evident by the XRD analysis [29]. In addition, PEG as surfactant also produced a relatively smaller CaO/MgO particles with high surface area and consequently enhanced the number of basic sites of the catalyst.

3.2.4 Nitrogen adsorption-desorption analysis

Surface area and pore size distribution of CaO/MgO were determined using nitrogen adsorption-desorption analysis. Figure 5 showed the N_2 isotherm of CaO/MgO catalysts was identified as the type II adsorption that indicated the behavior of nonporous material. At very low relative pressure P/Po, N_2 formed a monolayer adsorption on the surface with the volume of adsorbed N_2 significantly low for nonporous material. However, the volume of adsorbed N_2 for CaO/MgO-P was gradually increased until P/Po-0.9 suggesting the increase of surface area of the catalysts. At higher P/Po, the nitrogen adsorption-desorption showed hysterisis for capillary condensation which was due to the presence of inter-particle mesopores in CaO/MgO [39]. The hysteresis loop formed in the CaO/MgO catalyst was a type H-3 hysteresis loop that implied the presence of slit-shaped pores caused by the agglomeration of the particles [39].

The pore size distribution of CaO/MgO catalysts analyzed using the BJH method (Fig. 6) revealed the CaO/MgO produced from direct calcination of limestone, CaO/MgO-H from CHD without surfactant, and CaO/MgO-C using CTAB were nonporous material with traces of adsorption in microporous region, presumably due to the interaction between particles. However, it was apparent that CaO/MgO-P using PEG showed micropore and mesopore features with significant increase of the pore volume. It was suggested that the presence of mesopores originated from the inter-particle interaction which was evident by the hysterysis at a higher relative pressure P/Po [40]. CTAB and PEG surfactants were reported to facilitate the formation of mesopore structures for CaO catalysts [29]; however, the promotional effect of the surfactant was only observed when using PEG. BET surface area analysis also showed the increased of surface area when PEG was added during the CHD treatment at 39 m²/g, relative to the specific surface area of CaO/MgO produced from direct calcination of limestone at 900°C~9 m²/g. In the absence of surfactants and with the addition of CTAB surfactant, the CHD treatment showed no enhancement of the CaO/MgO surface area. It was suggested that PEG promoted the formation of small crystallites with interparticle mesoporosity to improve the specific surface area of the catalysts.

3.3 Characterization of NiO/CaO/MgO-P catalysts with XRD, FTIR, and FESEM

CaO reacted with CO_2 and H_2O in air to form the respective $CaCO_3$ and $Ca(OH)_2$ that compromised the activity as catalyst [41]; therefore, NiO was impregnated to CaOMgO-P to increase the stability of CaO. The XRD pattern of NiO/CaO/

Table 1 Textural properties of the CaO/MgO catalyst from natural limestone

Catalyst	Methods	Surface area (m²/g)	Pore volume (m³/g)	Size (nm)	Ca (%)	Mg (%)	Basicity mmol/g	Base strength
CaO/MgO	Calcination	9	0.0033	681	45	55	7.92	H_ = 15.0
CaO/MgO-H	CHD	3	0.0040	521	45	55	6.66	H_ = 15.0
CaO/MgO-C	CHD + CTAB	8	0.0025	391	47	53	6.98	H_ = 15.0
CaO/MgO-P	CHD + PEG	39	0.0322	377	52	48	7.8	H_ = 15.0

[1] CHD–calcination-hydration-dehydration

[2] BET surface area and pore volume (N_2 adsorption-desorption)

[3] Average particle size–particle size analyzer

[4] CaO, MgO from EDX analysis

[5] Basicity–Hammett indicator

Fig. 5 N$_2$ isotherm adsorption-desorption of CaO/MgO catalysts produced from direct calcination of limestone, CaO/MgO-H catalyst from CHD without surfactants, CaO/MgO-C catalyst from CHD using CTAB, and CaO/MgO-P catalyst catalyst from CHD using PEG
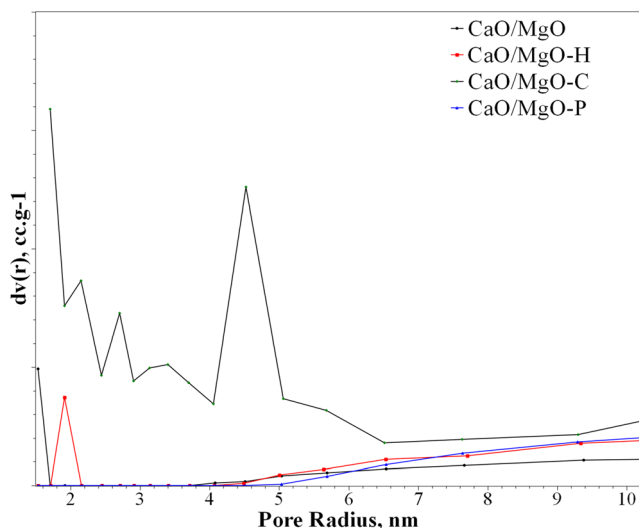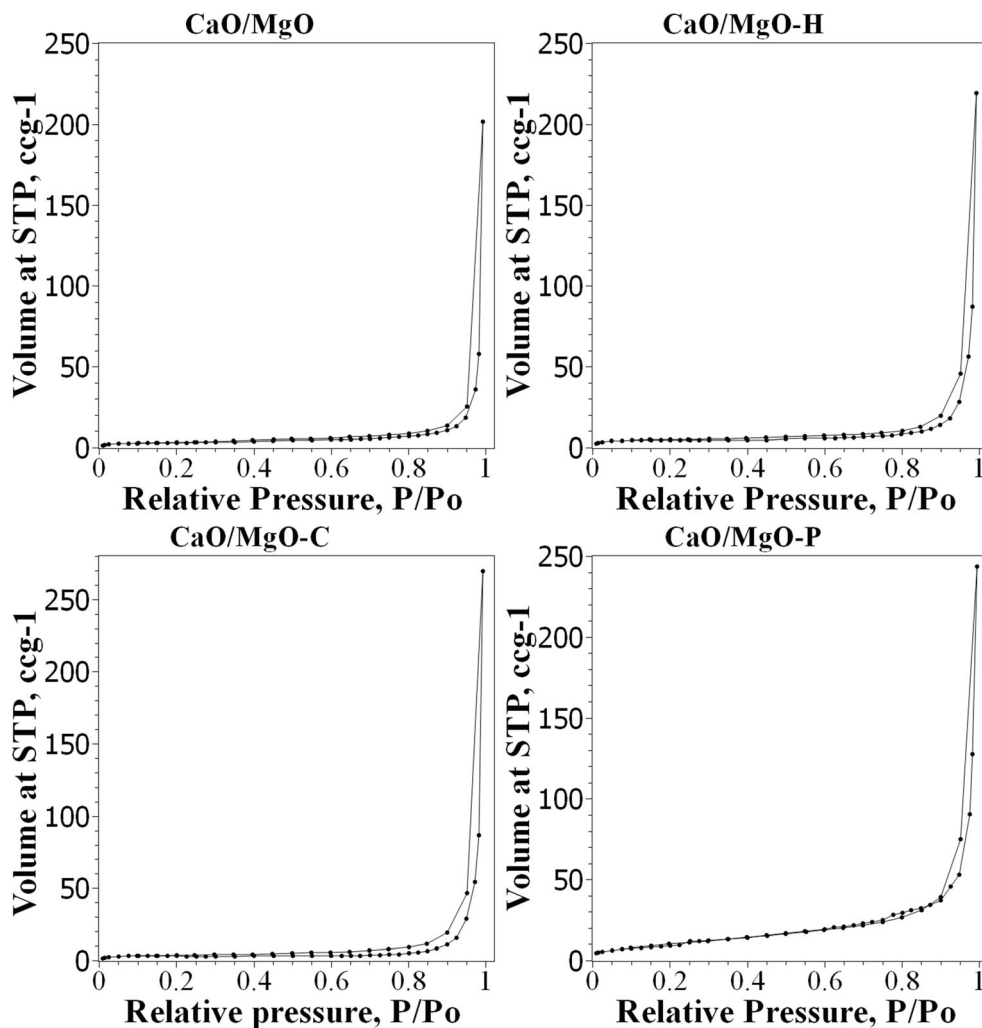
Fig. 6 Pore radius of CaO/MgO catalysts produced from direct calcination of limestone, CaO/MgO-H catalyst from CHD without surfactants, CaO/MgO-C catalyst from CHD using CTAB, and CaO/MgO-P catalyst from CHD using PEG

MgO at 2.5%, 5%, and 7.5% wt (Fig. 7) showed the absence of NiO peaks due to the characteristic peaks of NiO at 37.22°, 43.254°, 62.83°, and 75.35° 2θ (JCPDS card No-73-1523) was overlapped with the CaO and MgO peaks. However, the intensity of Ca(OH)$_2$ and calcite, CaCO$_3$, was significantly reduced with the increased loading of NiO, together with the increase intensity of CaO. The results suggested that nickel oxide stabilized CaO by inhibiting the reaction of CaO with CO$_2$ and H$_2$O for form calcite and Ca(OH)$_2$.

The infrared spectra of NiO/CaO/MgO-P in Fig. 8 showed the band observed at 3648 cm^{-1} was assigned to the vibrational stretching of –OH group attached in Ca(OH)$_2$ due to the hydrolysis of CaO to Ca(OH)$_2$ when exposed to air [42–44]. The intensity was significantly reduced following addition of NiO. XRD analysis also showed significant reduction of Ca(OH)$_2$ peak intensity with the increase of NiO loading (Fig. 7). The absorption band at 3448 cm^{-1} corresponded to the vibrational band of hydroxyl group from adsorbed water molecule [13, 42]. The absorption band at wavenumber 1419–1457 cm^{-1} and the narrow peak at 875 cm^{-1} were assigned to
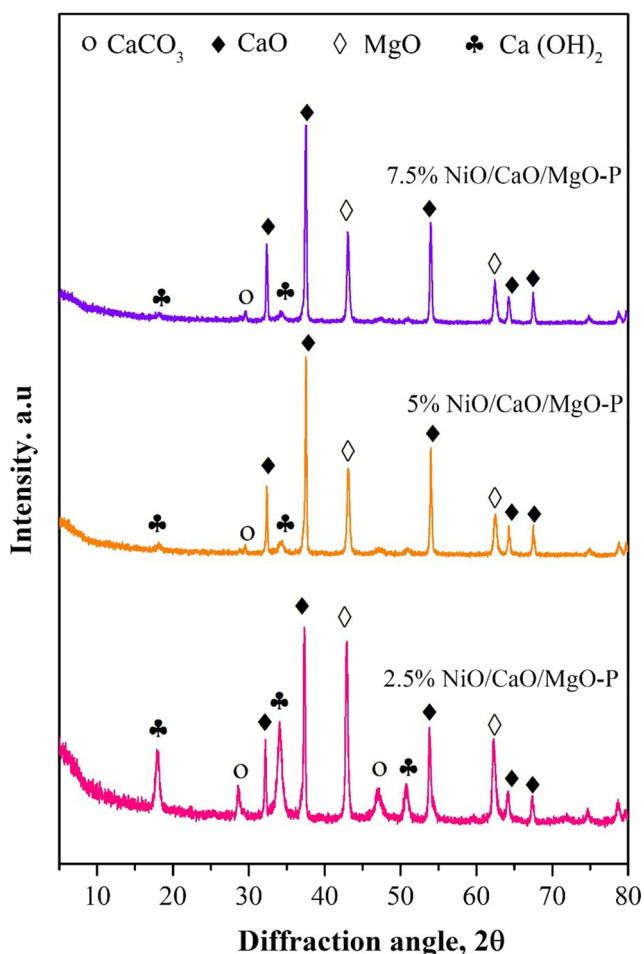
Fig. 7 XRD diffractogram of NiO/CaO/MgO-P

the asymmetric stretching vibrational peaks of the CO_3^{-2} group from calcite [42, 45] due to CO_2 chemisorption on the surface of the material [43]. Impregnation of NiO onto CaO/MgO-P catalyst reduced the formation of calcite as evidenced by the reduced intensity of 1421, 1457, and 875 cm^{-1} peaks for NiO/CaO/MgO-P catalyst in comparison to CaO/MgO-P. The presence of high amount of calcite in CaO reduced the number of acid sites for catalytic reaction [9].

3.4 Catalytic activity for transesterification of coconut oil

3.4.1 Catalytic activity of CaO/MgO

The activity of CaO/MgO catalysts for transesterification of coconut oil to biodiesel was carried out at 150°C, with the molar ratio of methanol to oil was 9:1. The conversion of oil, the biodiesel yield, and the free fatty acid production were summarized in Table 2. CaO/MgO produced from direct calcination of limestone at 900°C give 16.45% of conversion with 15.38% yield of biodiesel. Free fatty acid was also analyzed at 1.07%. Following CHD treatment to form

CaO/MgO-H, the activity was improved to give 23.93% of conversion with 20.95% of biodiesel yield. The presence of surfactants during the CHD treatment produced catalysts with enhanced conversion of coconut oil and selectivity towards biodiesel production. The selectivity of the methyl ester yield was increased from 87.5% in CaO/MgO-H to 96.04% in CaO/MgO-P. The selectivity towards free fatty acid also reduced to only 3.9% in CaO/MgO-P to give only ~ 1.95% of FFA yield. The addition of CTAB surfactant increased the conversion to 30.48% with the production of methyl ester also increased to 27.92%. CaO/MgO-P produced when using PEG further increased the conversion to 49.27% to give 47.32 % of biodiesel yield. The effect of CHD treatment to eliminate the large crystallites in CaO/MgO catalysts significantly enhanced the catalytic activity for transesterification reaction. The addition of surfactants during CHD treatment to form high surface area CaO/MgO not only enhanced the conversion of coconut oil, but also significantly improved the selectivity towards biodiesel production. The selectivity of the methyl ester yield was increased from 87.5% in CaO/MgO-H to 96.04% in CaO/MgO-P. The selectivity towards free fatty acid also reduced to 3.9% in CaO/MgO-P to give only ~ 1.95% of FFA yield.

Facile calcination-hydration-dehydration (CHD) method was carried out to upgrade the activity of CaO/MgO from limestone as catalyst for transesterification reaction. Elemental composition of the catalysts analyzed using EDX (Table 1) showed no significant differences on the composition of CaO and MgO and therefore the catalytic performances were correlated with the surface area and the particles size of the catalysts. Direct calcination of limestone produced low surface area and nonporous CaO/MgO with low activity as catalyst. Further hydration and dehydration with the presence of non-ionic PEG surfactant controlled the recrystallization of CaO/MgO to form small particles with enhanced surface area and porosity. It is interesting to see that although the ionic CTAB surfactant reduced the crystallite size of CaO/MgO, the surface area was still significantly low. PEG is a non-ionic surfactant with the presence of hydroxyl groups in the structures acted as electron donor to form hydrogen bond [46]. The hydroxyl group in PEG also formed a strong interaction with CaO/MgO crystallite to increase the dispersion that was crucial for the formation of smaller structures [46]. Hydration of CaO/MgO via sonication and microwave irradiation enhanced the dissolution; meanwhile, the addition of PEG created hydrophilic encapsulation layer on the surfaces. Hydrothermal method was known to produce uniform and well-dispersed crystallites [47, 48], and the presence of PEG provided hydrophilic layer to increase the repulsion that prevented agglomeration. Therefore, CHD treatment enhanced the dispersion of CaO/MgO particles, and the presence PEG surfactant further improved the surface area and the porosity of the catalysts.
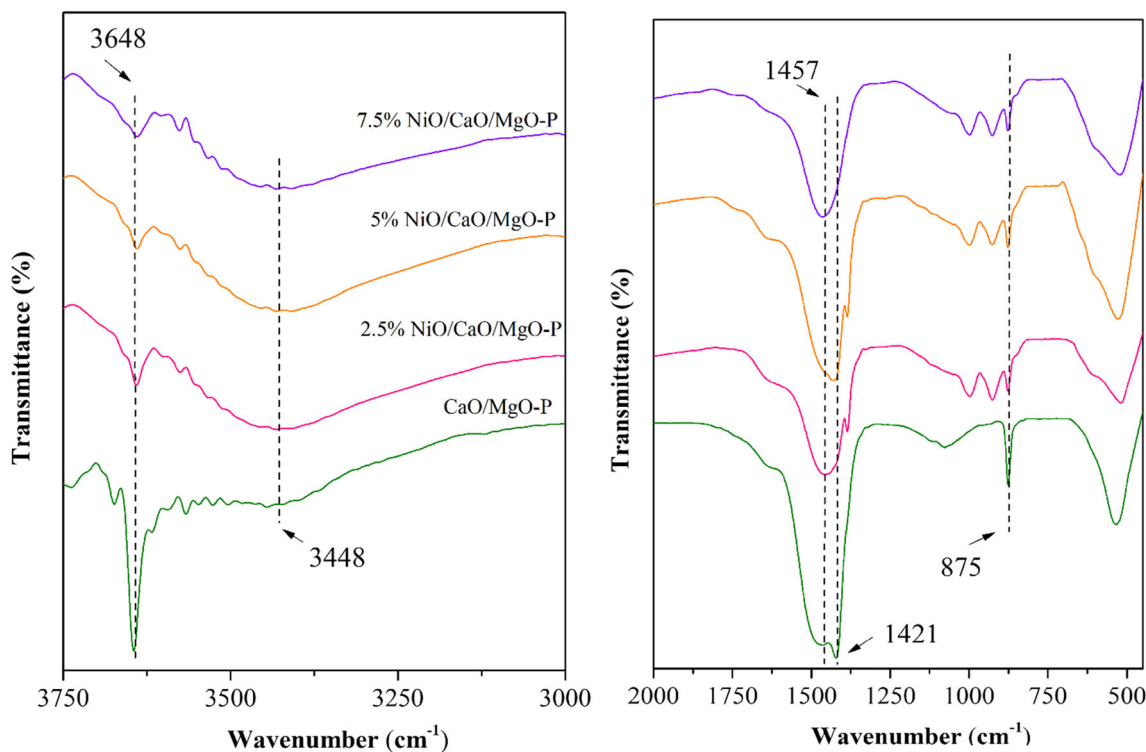
Fig. 8 Infrared spectra of CaO/MgO-P and NiO/CaO/MgO-P

3.4.2 Optimization of the amount of catalysts

Since the CaO/MgO produced with the addition of PEG displayed high activity for transesterification of coconut oil to biodiesel, the optimization of transesterification reaction condition was carried out using CaO/MgO-P, with the variation of the amount of catalysts at 0.625, 1.25, 2.5, 3.75, and 5% loading. Table 3 showed the catalytic data from transesterification of coconut oil when the reaction was carried out at 150°C and the ratio between methanol to oil was set at 1:9. The conversion of oil was increased from 31.92 to 75.44% when increasing the amount of catalyst from 0.625 to 2.5 wt% due to the addition of active sites for catalytic reaction [24]. The presence of basic sites facilitated the formation of highly reactive methoxy anion to react with carbonyl triglyceride group for the formation of biodiesel [7]. However, when the amount of catalyst was further increased to 3.75 and

5% wt, the yield significantly reduced to 63.10% and 49.6% respectively. Another factor that reduced the conversion was the viscosity of the reaction media. Further addition of the catalyst increased the viscosity and reduced the homogeneity of the reaction mixtures, consequently reducing the efficiency of the reaction [24].

3.4.3 Optimization of the ratio between oil to methanol for biodiesel synthesis

The efficiency of triglyceride conversion to methyl ester was significantly influenced by the concentration of methanol, and therefore methanol concentration was optimized by increasing the methanol to oil ratios from 1:3 to 1:15. The conversion of oil, biodiesel yield, and FFA production were summarized in Table 4. Biodiesel was produced at 61.94% when the ratio was 1:3 and further increasing the methanol to oil ratio at

Table 2 Transesterification of coconut oil on CaO/MgO catalyts

Catalyst	Conversion of oil (%)	Methyl ester selectivity (%)	FFA selectivity (%)	Methyl ester yield (%)	FFA yield (%)
CaO/MgO	16.45	93.5	6.5	15.38	1.07
CaO/MgO-H	23.93	87.5	12.4	20.95	2.98
CaO/MgO-C	30.48	91.6	8.4	27.92	2.56
CaO/MgO-P	49.27	96.04	3.9	47.32	1.95

*Molar ratio of methanol: oil 9:1, catalyst amount 5%, reaction time 3 h, and reaction temperature 150°C

Table 3 Transesterification reaction of coconut oil using CaO/MgO-P at different amount of catalysts

Catalyst loading (%)	Conversion of oil (%)	Methyl ester selectivity %	Methyl ester yield (%)	FFA yield (%)
0.625	31.92	90.13	28.77	3.15
1.25	79.51	86.39	68.69	10.82
2.50	75.44	97.98	73.92	1.52
3.75	63.10	96.80	61.08	2.02
5.00	49.56	94.56	47.05	2.51

[*] Catalyst: CaO/MgO-P, molar ratio of methanol: oil 9:1, reaction time 3 h, and reaction temperature 150°C

1:9 significantly enhanced the yield to 76.80%. High concentration of methanol in general shifted the reversible transesterification reaction to methyl ester production [12]. Methanol also facilitated the dispersion of the catalyst in the reaction media and reduced the mass transfer limitation [49]. However, high concentration of methanol also caused protonation of the carbonyl group of triglycerides that reduced the biodiesel yield as exhibited by slight reduction to 73.09% at 1:15 ratio. At higher methanol to oil molar concentrations, it reduced the viscosity and the concentration of oil. Low oil concentration was detrimental in transesterification reaction due to incomplete dispersion of methanol and also restricted the contact between reactants (oil and methanol) and the catalyst [50]. High concentration of methanol was also contributed to the increase of operational cost for biodiesel production due to the difficulty of separating the by-product glycerol from the methyl ester yield [12, 38].

3.4.4 Optimization of the reaction temperature for biodiesel synthesis

The effect of reaction temperature was investigated at 100–175°C while using 2.5 wt% of catalysts and 1:9 of methanol to oil ratio (Table 5). Biodiesel yield was increased from 76.51% at 100°C to 81.29% at 125°C. Further increasing the temperatures to 150°C and 175°C significantly reduced the catalytic transformation of coconut oil to biodiesel to only ~ 71.92% and 68.55%, respectively. Transesterification reaction of oil on heterogeneous catalyst was an endothermic reaction that

will benefit from high-temperature condition [14, 35]. Increasing the temperatures also enhanced the mass transfer of reactants to the active sites of the catalysts [51]. However at much higher temperatures, the biodiesel production was reduced due to the formation of excess free fatty acids which eventually reacted with CaO to produce soap [52]. The formation of soap from saponification reaction also reduced the mass transfer during the reaction [53]. Further decomposition of triglycerides to fatty acid was observed at 150°C and 175°C that consequently reduced the production of methyl esters.

3.5 The effect of NiO on CaO/MgO

CaO/MgO-P was impregnated with NiO to produce catalysts with acid-base functionality. The catalytic activity of NiO/CaO/MgO-P was determined at optimal reaction conditions (125 °C, 2.5% wt of catalyst, 3 h, and 1 methanol:9 oil mol ratios). NiO loading were varied at 2.5 % wt, 5.0 % wt, and 7.5% wt and the results were summarized in Table 6. The conversion of oil to biodiesel was significantly improved to 90.06% on 5% of NiO in comparison to CaO/MgO-P at 81.76% (Table 5). Impregnation of NiO also enhanced the selectivity of methyl ester at 99.68% to produce 89.77% of yield, and significantly reduced the FFA yield from 0.47% (Table 5) to 0.29% (Table 6). NiO was reported to have high activity than MgO and also increased the surface basicity of CaO for biodiesel production [54, 55]. The stability of CaO and presumably the water tolerance property were improved in the presence NiO evident by the XRD analysis of NiO/

Table 4 Biodiesel production from transesterification of coconut oil using CaO/MgO-P catalyst on the effect of methanol:oil ratios

Methanol:oil	Conversion (%)	Methyl ester yield (%)	Methyl ester selectivity (%)	FFA (%)
1:3	62.21	61.94	99.56	0.27
1:6	69.14	68.36	98.87	0.78
1:9	77.61	76.80	98.96	0.81
1:12	74.04	72.47	97.88	1.57
1:15	74.00	73.09	98.77	0.91

[*] Catalyst: CaO/MgO-P, the amount of catalyst was 2.5 wt%, the reaction temperature was 150°C, and the reaction time was 3 h

Table 5 The effect of reaction temperatures for biodiesel production

Temperature (°C)	Conversion (%)	Methyl ester yield (%)	Methyl ester selectivity (%)	FFA yield (%)
100	77.83	76.51	98.30	1.32
125	81.76	81.29	99.42	0.47
150	72.32	71.29	98.58	1.03
175	70.55	68.55	97.17	2.00

[*] The transesterification was carried out using 2.5 wt% CaO/MgO-P catalyst at the molar ratio of oil:methanol of 1:9, for 3 h

CaO/MgO that showed the disappearances of $Ca(OH)_2$ and $CaCO_3$ peaks in comparison to the CaO/MgO catalyst [54]. Analysis of the biodiesel exhibited similar methyl esters composition from CaO/MgO-P and 5%NiO/CaO/MgO-P catalysts; however, the yield and the selectivity of methyl ester were significantly improved in the presence of NiO. Free fatty acids in the form of octanoic acid, capric acid, myristic acid, caproic acid, and oleic acid were analyzed from CaO/MgO-P; however, the presence of NiO co-catalyst only produced lauric acid (Fig. 9 inset). The results suggest the ability of NiO to catalyze esterification of fatty acids to methyl esters.

The mechanism of transesterification using NiO/CaO/MgO-P catalyst started with the reaction of hydroxyl group in methanol with the basic sites presumably on CaO and MgO surfaces to form methoxide species, CH_3O^-, via deprotonation reaction [56]. Triglyceride adsorbed on CaO consequently weakens the C=O bond strength for the reaction with methoxide to form methyl esters. High concentration of fatty acids decreased the basicity and poisoned the catalysts [57]. Biodiesel was also produced from free fatty acids in the oil by the esterification with methoxide species to form methyl ester; however, the reaction required the presence of acid catalyst [58]. It is interesting to note that NiO also has acid-base properties with large isoelectric point of 8.3–10.3 [59]. There is a possibility that modification of NiO in CaO/MgO-P may be contributed to the formation of both acid and base sites [60]. NiO was reported to produce bifunctional catalysts with strong basicity and moderate acidity when impregnated on $CaO/SiO_2/Al_2O_3$ that enhanced the activity for deoxygenation reaction [61]. The bifunctional acid-base catalyst can simultaneously perform esterification of free fatty acids and transesterification of triglycerides. The acid and base sites on NiO/CaO/MgO were immobilized and insoluble in the reaction medium (methanol), thus restricting the interaction that can cause neutralization unlike in homogeneous system. In esterification of free fatty acid, NiO acted as Lewis acid sites to activate the free fatty acids conversion to biodiesel. Synergistic effect between basicity and acidity increased the formation of fatty acid methyl esters in the mild condition and accelerated the process of fatty acid esterification into methyl esters [56]. Free fatty acids were converted to methyl esters presumably via C=O bond activation on NiO to transform the carbon carbonyl into active carbon intermediates. The active carbon species was subsequently reacted with methoxide to produce methyl ester. Proposed mechanism of transesterification of triglycerides and esterification of free fatty acids to biodiesel on NiO/CaO/MgO reaction were illustrated in Fig. 10.

3.6 Properties and component of biodiesel

Table 7 summarized the properties of biodiesel from coconut oil produced using CaO/MgO-P and NiO/CaO/MgO-P. The results were also compared with the properties of biodiesel according to ASTM D6751 standard and biodiesel from coconut oil reported by Nakpong et al., (2010) [52]. Biodiesel derived from coconut oil has the density of 0.86–0.87 g/cm^3 which was within the standard and also comparable with the reported studies [8, 52]. The viscosity of biodiesel from coconut oil was determined at ~1.88–1.93 mm^2/s, significantly lower than the biodiesel derived from soybean oil (4.08 mm^2/s) [52]. Methyl ester component analyzed using GC-

**Table 6** The effect NiO loading on CaO/MgO activity for biodiesel production

Sample	Conversion (%)	Methyl ester yield (%)	Methyl ester selectivity (%)	FFA yield (%)
2.5% NiO/CaO/MgO$^{(2)}$-P	84,63	84.12	99.39	0,14
5% NiO/CaO/MgO$^{(2)}$-P	90,06	89.77	99.68	0.29
7.5% NiO/CaO/MgO$^{(2)}$-P	88.26	87,91	99.60	0.35

[*] Transesterification conditions: catalyst loading: 2.5 wt%, ratio of methanol to oil: 9:1 and reaction temperature: 125°C, reaction time 3 h

Fig. 9 Analysis of biodiesel composition produced using CaO/MgO-P and NiO/CaO/MgO-P
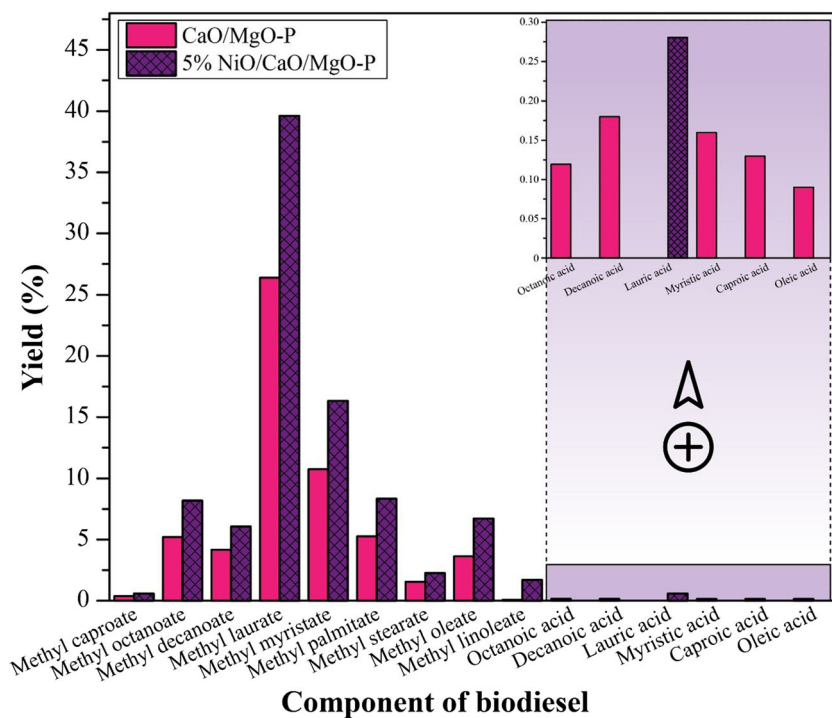
Fig. 10 Proposed reaction mechanism for biodiesel production using NiO/CaO/MgO-P catalyst
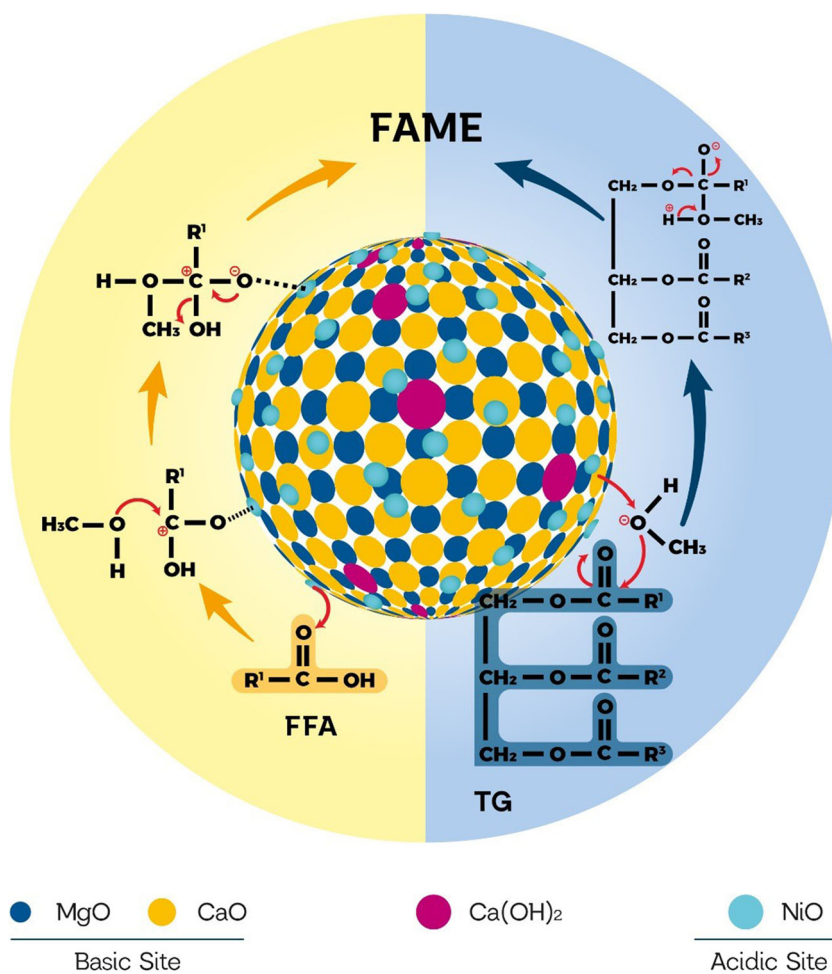
Table 7 Properties of biodiesel from transesterification of coconut using CaO/MgO-P and NiO/CaO/MgO-P catalysts

| Properties of biodiesel	ASTM D6751	Synthesized biodiesel by CaO/MgO-P	Synthesized biodiesel by 5%NiO/CaO/MgO-P	Nakpong et al., (2010)
Density (g/cm^3)	0.86–0.90	0.87	0.86	0.87
Viscosity (mm^2/s)	1.9–6.0	1.88	1.93	2.9
Flashpoint (°C)	100–170	132	137	191
Number of acids (mg KOH/g)	< 0.8	0.22	0.27	0.29
Carbon residue (%)	< 0.3	0.21	0.22	0.24

[*] Reaction conditions: catalyst loading: 2.5 wt%, ratio of methanol to oil: 9:1, reaction temperature: 125°C, and reaction time 3 h

MS (Fig. 11) indicated that ~50% of the methyl esters were in the form of short chained compounds such as methyl laurate, methyl myristate, methyl decanoate, and methyl caproate, contributing to the low viscosity of biodiesel [52]. Acidity, flashpoint, and number of acids were also determined within the standard properties of biodiesel. The carbon residues of the biodiesel were significantly low indicating the potential of biodiesel derived from coconut oil to reduce knocks when used in diesel engines [8].

4 Conclusion

Catalytic upgrading of CaO/MgO from limestone was achieved using calcination-hydration-dehydration (CHD) method without removal of MgO. Direct calcination of limestone produced CaO/MgO with low surface area resulting in low activity towards transesterification reaction. The presence of PEG surfactant during CHD method produced CaO/MgO with high surface area, porosity, and basicity that were responsible for the enhanced activity towards transesterification of coconut oil to biodiesel. CHD method in general reduced the presence of large CaO/MgO crystallites resulting from direct calcination of limestone at 900°C. The addition of CTAB and PEG surfactants further reduced the crystallite size, but the surface area only increased when using PEG. Optimization of the reaction temperatures, the methanol to oil ratios, and the amount of catalysts showed that the optimum conditions for the transesterification reaction were obtained when the amount of catalyst was 2.5% w/w at 1:9 of methanol to oil ratio and the reaction temperature was 125°C to give ~ 81.29% of biodiesel yield. Impregnation of NiO on CaO/MgO effectively increased the production of methyl esters and reduced the FFA formation. NiO introduced acid-base functionality to further enhance the esterification of free fatty acids to methyl esters. Biodiesel derived from coconut oil exhibited the physicochemical properties that were within the ASTM D6751 standard although the viscosity was
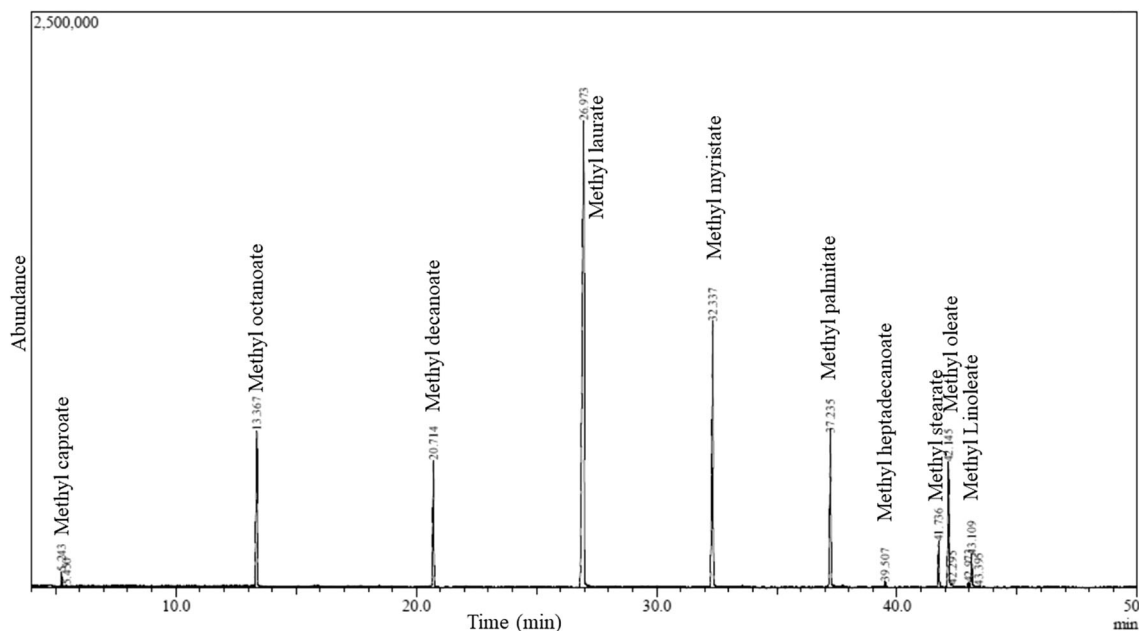
Fig. 11 GC chromatogram of methyl ester in biodiesel

significantly lower than the standard parameters due to the presence of light carbon-chained methyl esters.

References

1. Mansir N, Rashid U, Teo SH, Taufiq-Yap YH, Alsultan GA, Tan YP, Saiman MI (2017) Modified waste egg shell derived bifunctional catalyst for biodiesel production from high FFA waste cooking oil. A review. Renew Sust Energ Rev 82:3645–3655

2. Sekoai PT, Ouma CNM, du Preez SP, Modisha P, Engelbrecht N, Bessarabov DG, Ghimire A (2019) Application of nanoparticles in biofuels: an overview. Fuel 237:380–397

3. Lee HV, Taufiq-Yap YH (2015) Optimization study of binary metal oxides catalyzed transesterification system for biodiesel production. Process Saf Environ Prot 94:430–440

4. Ur W, Fatima A, Hakeem A, Athar M, Zain M, Ahmad N, Halder G (2019) Biodiesel synthesis from eucalyptus oil by utilizing waste egg shell derived calcium based metal oxide catalyst. Process Saf Environ Prot 122:313–319

5. Yuan S, Periasamy LAP, Ming C, Goh H, Hua Y (2020) Journal of Industrial and Engineering Chemistry Biodiesel synthesis using natural solid catalyst derived from biomass waste — A review. J Ind Eng Chem 81:41–60

6. Khalili RGR, Salehi DY (2016) Waste animal bone as support for CaO impregnation in catalytic biodiesel production from vegetable oil. Waste Biomass Valor 7:527–532

7. Roschat W, Phewphong S, Thangthong A, Moonsin P, Yoosuk B, Kaewpuang T, Promarak V (2018) Catalytic performance enhancement of CaO by hydration-dehydration process for biodiesel production at room temperature. Energy Convers Manag 165:1–7

8. Zareh P, Asghar A, Ghobadian B (2017) Comparative assessment of performance and emission characteristics of castor , coconut and waste cooking based biodiesel as fuel in a diesel engine. Energy 139:883–894

9. Marinkovi DM, Stankovi MV, Veli AV, Avramovi JM, Miladinovi MR, Stamenkovi OO, Veljkovi VB, Jovanovi M (2016) Calcium oxide as a promising heterogeneous catalyst for biodiesel production : Current state and perspectives. Renew Sust Energ Rev 56:1387–1408

10. Maneerung T, Kawi S, Dai Y, Wang CH (2016) Sustainable biodiesel production via transesterification of waste cooking oil by using CaO catalysts prepared from chicken manure. Energy Convers Manag 123:487–497

11. Mishra VK, Goswami R (2017) A review of production , properties and advantages of biodiesel. Biofuels 0:1–17

12. Borah MJ, Das A, Das V, Bhuyan N, Deka D (2019) Transesterification of waste cooking oil for biodiesel production catalyzed by Zn substituted waste egg shell derived CaO nanocatalyst. Fuel 242:345–354

13. Gupta AR, Rathod VK (2018) Waste cooking oil and waste chicken eggshells derived solid base catalyst for the biodiesel production: optimization and kinetics. Waste Manag 79:169–178

14. Xie W, Wang H (2020) Synthesis of heterogenized polyoxometalate-based ionic liquids with Brönsted-Lewis acid sites : a magnetically recyclable catalyst for biodiesel production from low-quality oils. J Ind Eng Chem 87:162–172

15. Li X, Zuo Y, Zhang Y, Fu Y, Guo Q (2013) In situ preparation of K 2 CO 3 supported Kraft lignin activated carbon as solid base catalyst for biodiesel production. Fuel 113:435–442

16. Teo SH, Islam A, Masoumi HRF, Taufiq-Yap YH, Janaun J, Chan ES, Khaleque MA (2017) Effective synthesis of biodiesel from *Jatropha curcas* oil using betaine assisted nanoparticle heterogeneous catalyst from eggshell of *Gallus domesticus*. Renew Energy 111:892–905

17. Maneerung T, Kawi S, Wang CH (2015) Biomass gasification bottom ash as a source of CaO catalyst for biodiesel production via transesterification of palm oil. Energy Convers Manag 92:234–243

18. Ketcong A, Meechan W, Naree T, Seneevong I, Winitsorn A, Butnark S, Ngamcharussrivichai C (2014) Journal of Industrial and Engineering Chemistry Production of fatty acid methyl esters over a limestone-derived heterogeneous catalyst in a fixed-bed reactor. J Ind Eng Chem 20:1665–1671

19. Suprapto, Fauziah TR, Sangi MS, Oetami TP, Qoniah I, Prasetyoko D (2016) Calcium oxide from limestone as solid base catalyst in transesterification of Reutealis trisperma oil. Indones J Chem 16:208–213

20. Mohadi R, Anggraini K, Riyanti F, Lesbani A (2016) Preparation Calcium oxide from chicken eggshells. SJE 1:32–35

21. Boey PL, Ganesan S, Maniam GP, Khairuddean M (2012) Catalysts derived from waste sources in the production of biodiesel using waste cooking oil. Catal Today 190:117–121

22. Lei S, Gan Y, Cao Z, Wang S, Zhong H (2020) The preparation of high purity MgO and precision separation mechanism of Mg and Ca from dolomite. Mining, Metall Explor 37:1221–1230

23. Akarsu H, Yildirim M (2008) Leaching rates of icel-yavca dolomite in hydrochloric acid solution. Miner Proc Extr Met Rev 29:42–56

24. Rabie AM, Shaban M, Abukhadra MR, Hosny R, Ahmed SA, Negm NA (2019) Diatomite supported by CaO / MgO nanocomposite as heterogeneous catalyst for biodiesel production from waste cooking oil. J Mol Liq 279:224–231

25. Wen L, Guan Y, Han H, Hu S, Wang Y (2009) Preparation of mesoporous nanosized KF/CaO–MgO Catalyst and its application for biodiesel production by transesterification. Catal Lett 131:574–578

26. Yang H, Dong H, Zhang T, Zhang Q, Zhang G, Wang P, Liu Q (2019) Calcined dolomite : an efficient and recyclable catalyst for synthesis of α , β -unsaturated carbonyl compounds. Catal Lett 149:778–787

27. Xu D, Feng J, Che S (2014) An insight into the role of the surfactant CTAB in the formation of microporous molecular sieves. Dalt Trans 43:3612–3617

28. Bastakoti BP, Ishihara S, Leo SY, Ariga K, Wu KCW, Yamauchi Y (2014) Polymeric micelle assembly for preparation of large-sized mesoporous metal oxides with various compositions. Langmuir 30:651–659

29. Liu C, Zhang L, Deng J, Mu Q, Dai H, He H (2008) Surfactant-aided hydrothermal synthesis and carbon dioxide adsorption behavior of three-dimensionally mesoporous calcium oxide single-crystallites with tri-, tetra-, and hexagonal morphologies. J Phys Chem C 112:19248–19256

30. Ahmadi P, Alamolhoda S, Mirkazemi SM (2018) Cetyltrimethylammonium bromide (CTAB) surfactant-assisted synthesis of $BiFeO_3$ nanoparticles by sol-gel auto-combustion method. J Supercond Nov Magn 31:3307–3314

31. Rajisha KR, Deepa B, Pothan LA, Thomas S (2011) Thermomechanical and spectroscopic characterization of natural fibre composites. In: Interface Eng Nat Fibre Compos, Maximum Perform. Elsevier, pp 241–274

32. Jindapon W, Ngamcharussrivichai C (2018) Heterogeneously catalyzed transesterification of palm oil with methanol to produce biodiesel over calcined dolomite: the role of magnesium oxide. Energy Convers Manag 171:1311–1321

33. Hu S, Wang Y, Han H (2011) Utilization of waste freshwater mussel shell as an economic catalyst for biodiesel production. Biomass Bioenergy 35:3627–3635

34. Gunasekaran S, Anbalagan G (2011) Thermal decomposition of natural dolomite. Inorg Mater 47:1372–1377

35. Roschat W, Siritanon T, Yoosuk B, Promarak V (2016) Biodiesel production from palm oil using hydrated lime-derived CaO as a low-cost basic heterogeneous catalyst. Energy Convers Manag 108:459–467

36. Deng J, Zhang L, Liu C, Xia Y, Dai H (2011) Single-crystalline mesoporous CaO supported Cr – V binary oxides : highly active catalysts for the oxidative dehydrogenation of isobutane. Catal Today 164:347–352

37. Xie W, Yang X, Fan M (2015) Novel solid base catalyst for biodiesel production : Mesoporous SBA-15 silica immobilized with 1 , 3-dicyclohexyl-2-octylguanidine. Renew Energy 80:230–237

38. Maleki H, Kazemeini M, Larimi AS, Khorasheh F (2017) Transesteri fi cation of canola oil and methanol by lithium impregnated CaO – La 2 O 3 mixed oxide for biodiesel synthesis. J Ind Eng Chem 47:399–404

39. Lingling Q, Xu T, Zhaofeng W, Xinshan P (2017) Pore characterization of different types of coal from coal and gas outburst disaster sites using low temperature nitrogen adsorption approach. Int J Min Sci Technol 27:371–377

40. Bolbukh KFY, Podkościelna MGB, Gawdzik MGB (2019) Synthesis and characterization of mesoporous polymeric microspheres of methacrylic derivatives of aromatic thiols. Adsorption 25:429–442

41. Abdullah AZ, Yaacob MH, Basir NI (2020) Synergy between oxides of Ni and Ca for selective catalytic lactic acid synthesis from glycerol in a single step process. J Ind Eng Chem 85:282–288

42. Syazwani ON, Teo SH, Islam A, Taufiq-Yap YH (2017) Transesterification activity and characterization of natural CaO derived from waste venus clam (Tapes belcheri S.) material for enhancement of biodiesel production. Process Saf Environ Prot 105: 303–315

43. Barros FJS, Moreno-Tost R, Cecilia JA, Ledesma-Muñoz AL, de Oliveira LCC, Luna FMT, Vieira RS (2017) Glycerol oligomers production by etherification using calcined eggshell as catalyst. Mol Catal 433:282–290

44. Boro J, Konwar LJ, Deka D (2014) Transesteri fi cation of non edible feedstock with lithium incorporated egg shell derived CaO for biodiesel production. Fuel Process Technol 122:72–78

45. Đokić-Stojanović DR, Veselinović LM, Stamenković OS et al (2018) Optimization of CaO-catalyzed sunflower oil methanolysis with crude biodiesel as a cosolvent. Renew Energy 242:345–354

46. Morikawa H, Koike S, Saiki M, Saegusa Y (2008) Synthesis and characterization of the PEG-based nonionic surfactants endowed with carboxylic acid moiety at the hydrophobic terminal. J Polym Sci Part A Polym Chem 46:8206–8212

47. Zhao HY, Wang YF, Zeng JH (2008) Hydrothermal synthesis of uniform cuprous oxide microcrystals with controlled morphology. Cryst Growth Des 8:3731–3734

48. Guan J, Zhang Z, Ji J, Dou M, Wang F (2017) Hydrothermal synthesis of highly dispersed Co_3O_4 nanoparticles on biomass-derived nitrogen-doped hierarchically porous carbon networks as an efficient bifunctional electrocatalyst for oxygen reduction and evolution reactions. ACS ApplMater Interfaces 9:30662–30669

49. Fadhil AB, Al-Tikrity ETB, Khalaf AM (2018) Transesterification of non-edible oils over potassium acetate impregnated CaO solid base catalyst. Fuel 234:81–93

50. Badnore AU, Jadhav NL, Pinjari DV, Pandit AB (2018) Efficacy of newly developed nano-crystalline calcium oxide catalyst for biodiesel production. Chem Eng Process Process Intensif 133:312–319

51. Mansir N, Teo SH, Rashid U, Taufiq-Yap YH (2018) Efficient waste Gallus domesticus shell derived calcium-based catalyst for biodiesel production. Fuel 211:67–75

52. Nakpong P, Woottthikanokkhan S (2010) High free fatty acid coconut oil as a potential feedstock for biodiesel production in Thailand. Renew Energy 35:1682–1687

53. Dharma M, Irawan C, Ristianingsih Y (2018) A cleaner process for biodiesel production from waste cooking oil using waste materials as a heterogeneous catalyst and its kinetic study. J Clean Prod 195: 1249–1258

54. Teo SH, Rashid U, Taufiq-Yap YH (2014) Biodiesel production from crude Jatropha Curcas oil using calcium based mixed oxide catalysts. Fuel 136:244–252

55. Ariffin MI, Abdullah N, Bahruji H, Mohd Kasim NA, Abdul Halim N, Yun Hin TY (2019) Optimization of biodiesel production from Chlorella Vulgaris using CuO, NiO and MgO on zeolite 4A catalysts. In: J Phys Conf Ser, Institute of Physics Publishing, pp 12065

56. Pandey LM, Saxena V, Chandra P, Baranwal A, Sharma S (2018) Engineered nanoporous materials mediated heterogeneous catalysts and their implications in biodiesel production. Mater Sci Energy Technol 1:11–21

57. Coman SM, Parvulescu VI (2013) Heterogeneous catalysis for biodiesel production. In: Role Catal Sustain Prod, Bio Fuels Bio Chemicals. Elsevier Inc, pp 93–136

58. Ichihara K, Fukubayashi Y (2010) Preparation of fatty acid methyl esters for gas-liquid chromatography. J Lipid Res 51:635–640

59. Kung HH (1989) Transition metal oxides: surface chemistry and catalysis. In: Stud Surf Sci Catal, 1st edn. Elsevier Inc, pp 1–282

60. Asikin-mijan N, Lee HV, Taufiq-yap YH, Abdulkrem-alsultan G, Mastuli MS (2017) Optimization study of SiO 2 -Al 2 O 3 supported bifunctional acid – base NiO-CaO for renewable fuel production using response surface methodology. Energy Convers Manag 141: 325–338

61. Asikin-mijan N, Lee HV, Marliza TS, Tau YH (2018) Pyrolyticdeoxygenation of triglycerides model compound and non-edible oil to hydrocarbons over SiO 2 -Al 2 O 3 supported NiO-CaO catalysts. J Anal Appl Pyrolysis 129:221–230